JOURNAL OF AIRCRAFT
Vol. 41, No. 5, September–October 2004

Lifting-Line Analysis of Roll Control and Variable Twist

W. F. Phillips,* N. R. Alley,† and W. D. Goodrich†
Utah State University, Logan, Utah 84322-4130

A more practical form of an analytical solution that can be used to predict the roll response for a wing of arbitrary planform with arbitrary spanwise variation of control surface deflection and wing twist is presented. This infinite series solution is based on Prandtl's classical lifting-line theory, and the Fourier coefficients are presented in a form that depends only on wing geometry. The solution can be used to predict rolling and yawing moments as well as the lift and induced drag, which result from control surface deflection, rolling rate, and wing twist. The analytical solution can be applied to wings with conventional ailerons or to wings utilizing wing-warping control. The method is also applied to full-span twisting control surfaces, named "twisterons," which can be simultaneously used to provide roll control, high-lift, and minimum induced drag.

Nomenclature

A_n = coefficients in the infinite series solution to the lifting-line equation
a_n = planform contribution to the coefficients in the infinite series solution to the lifting-line equation
b = wingspan
b_n = twist contribution to the coefficients in the infinite series solution to the lifting-line equation
C_{Di} = induced-drag coefficient
C_L = lift coefficient
$C_{L,\alpha}$ = wing lift slope
$\tilde{C}_{L,\alpha}$ = airfoil-section lift slope
C_{L,δ_f} = change in wing lift coefficient with respect to flap deflection
C_{L,δ_t} = change in wing lift coefficient with respect to twisteron deflection
C_ℓ = rolling-moment coefficient
$C_{\ell,\bar{p}}$ = change in rolling-moment coefficient with respect to dimensionless rolling rate
$C_{\ell,\delta}$ = change in rolling-moment coefficient with respect to control surface deflection
C_m = pitching moment coefficient
C_{m,δ_t} = change in pitching-moment coefficient with respect to twisteron deflection
C_n = yawing moment coefficient
$C_{n,\bar{p}}$ = change in yawing moment coefficient with respect to dimensionless rolling rate
$C_{n,\delta}$ = change in yawing moment coefficient with respect to control surface deflection
c = local wing section chord length
c_f = local flap chord length
c_n = roll control contribution to the coefficients in the infinite series solution to the lifting-line equation
$\tilde{D}_i$ = local section induced drag
d_n = rolling rate contribution to the coefficients in the infinite series solution to the lifting-line equation
$\tilde{L}$ = local section lift
p = rolling rate, positive right wing down
$\bar{p}$ = dimensionless rolling rate, $pb/2V_\infty$
$\bar{p}_0$ = equilibrium dimensionless rolling rate
R_A = wing aspect ratio
R_T = wing taper ratio
S = wing planform area
V_∞ = magnitude of the freestream velocity
y = spanwise coordinate from mid-span, positive right
y_{ar} = spanwise coordinate of aileron root
y_{at} = spanwise coordinate of aileron tip
α = spanwise variation in local geometric angle of attack relative to the freestream
α_i = spanwise variation in local induced angle of attack
α_{L0} = spanwise variation in local zero-lift angle of attack
Γ = local spanwise section circulation distribution
Δ = modifier indicating an incremental change
δ = total or maximum control surface deflection angle
δ_a = total or maximum aileron deflection angle, positive right side trailing edge down
δ_f = total or maximum flap deflection angle, positive trailing edge down
δ_t = total or maximum flap twist angle, washout positive
ε_f = local airfoil-section flap effectiveness
θ = change of variables for the spanwise coordinate
κ_{DL} = lift-washout contribution to the induced drag factor
$\kappa_{D\Omega}$ = washout contribution to the induced drag factor
$\kappa_{\ell\bar{p}}$ = roll damping factor
ρ = air density
χ = spanwise control surface distribution function for flaps or ailerons
Ω = maximum total symmetric twist angle, geometric plus aerodynamic, washout positive
ω = spanwise symmetric twist distribution function

Introduction

FOR a finite wing with no sweep or dihedral, an analytical solution to Prandtl's classical lifting-line equation[1,2] can be obtained in terms of a Fourier sine series. From this solution the spanwise circulation distribution is expressed as

$$\Gamma(\theta) = 2bV_\infty \sum_{n=1}^{\infty} A_n \sin(n\theta) \tag{1}$$

where

$$\theta = \cos^{-1}(-2y/b) \tag{2}$$

and the Fourier coefficients A_n satisfy the relation

$$\sum_{n=1}^{\infty} A_n \left[\frac{4b}{\tilde{C}_{L,\alpha} c(\theta)} + \frac{n}{\sin(\theta)} \right] \sin(n\theta) = \alpha(\theta) - \alpha_{L0}(\theta) \tag{3}$$

Presented as Paper 2003-4061 at the AIAA 21st Applied Aerodynamics Conference, Orlando, FL, 23 June 2003; received 14 July 2003; revision received 14 October 2003; accepted for publication 14 October 2003.

*Professor, Mechanical and Aerospace Engineering Department, 4130 Old Main Hill. Member AIAA.
†Graduate Student, Mechanical and Aerospace Engineering Department, 4130 Old Main Hill. Member AIAA.

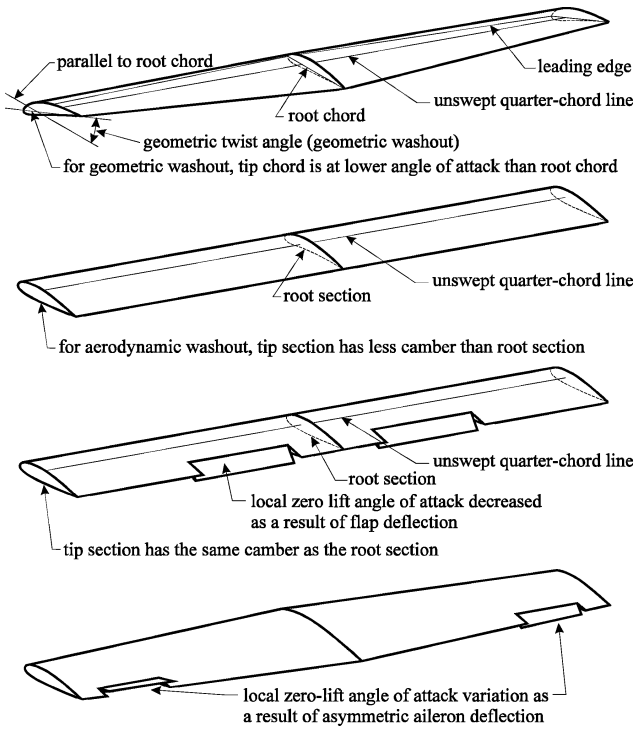

Fig. 1 Examples of geometric and aerodynamic twist.

In Eq. (3) α and α_{L0} are allowed to vary with the spanwise coordinate to account for various forms of geometric and aerodynamic twist, such as the examples shown in Fig. 1. In addition to fixed washout and control surface deflection, such twist can be used to describe the asymmetric wing warping sometimes used for roll control. It can also be used to model the spanwise variation in section angle of attack that results from a finite rolling rate. For a given wing geometry and operating condition, the planform shape, airfoil-section lift slope, geometric angle of attack, and zero-lift angle of attack are all known functions of spanwise position. The only unknowns in Eq. (3) are the Fourier coefficients A_n. Historically, these coefficients have usually been evaluated from collocation methods. Typically, the series is truncated to a finite number of terms, and the coefficients in the finite series are evaluated by requiring Eq. (3) to be satisfied at a number of spanwise locations equal to the number of terms in the series. A very straightforward method was first presented by Glauert.[3] The most popular method, based on Gaussian quadrature, was originally presented by Multhopp.[4] Another method, based on Fourier series expansion of wing geometry, was first proposed by Lotz[5] and is described by Karamcheti.[6] These methods give identical results in the limit as the number of terms carried in the infinite series becomes large. Furthermore, as pointed out by Bertin[7] the methods converge at about the same rate and give similar accuracy for the same level of truncation. Results presented here do not depend on the method of solution.

For a wing with no rolling rate and neither geometric nor aerodynamic twist, α and α_{L0} are both independent of θ, and the Fourier coefficients in Eq. (3) can be written as

$$A_n \equiv a_n(\alpha - \alpha_{L0}) \tag{4}$$

which reduces Eq. (3) to

$$\sum_{n=1}^{\infty} a_n \left[\frac{4b}{\tilde{C}_{L,\alpha} c(\theta)} + \frac{n}{\sin(\theta)} \right] \sin(n\theta) = 1 \tag{5}$$

The Fourier coefficients obtained from Eq. (5) depend only on the airfoil-section lift slope and the planform shape of the wing. They are independent of operating conditions. For a more detailed presentation of lifting-line theory, see Bertin,[7] Anderson,[8] Katz and Plotkin,[9] Kuethe and Chow,[10] or McCormick.[11]

Solution with Wing Twist, Control Surface Deflection, and Rolling Rate

The procedure commonly used for lifting-line analysis of wings having some form of geometric and/or aerodynamic twist is based on Eqs. (1–3) and requires evaluating separate sets of the Fourier coefficients A_n for several angles of attack and control surface deflections. Glauert,[3] Bertin,[7] and Kuethe and Chow[10] present the details of this procedure for wings having a continuous spanwise distribution of geometric and/or aerodynamic twist. Application of the procedure to evaluate the spanwise lift distribution resulting from the step change in aerodynamic angle of attack that is caused by the deflection of partial-span trailing-edge flaps and/or ailerons was presented by Munk,[12,13] Glauert,[14] Hartshorn,[15] Pearson,[16,17] and Pearson and Jones.[18] Because a fairly large number of terms must be carried to adequately represent the Fourier expansion of a step function, lifting-line analysis for wings with deflected flaps and ailerons was extremely laborious, prior to the development of the digital computer. This labor was amplified by the fact that the procedure required evaluating a complete set of Fourier coefficients for each angle of attack and flap deflection angle investigated.

A more practical form of this solution can be obtained by using the change of variables presented by Phillips.[19,20] Here we let

$$\alpha(y) - \alpha_{L0}(y) \equiv (\alpha - \alpha_{L0})_{\text{root}} - \Omega\omega(y) + \delta\chi(y) + py/V_\infty \tag{6}$$

where

$$\Omega \equiv [(\alpha - \alpha_{L0})_{\text{root}} - (\Delta\alpha - \Delta\alpha_{L0})_{\max}]_{\text{twist}} \tag{7}$$

and $\omega(y)$ is the spanwise symmetric twist distribution function,

$$\omega(y) \equiv \left[\frac{\Delta\alpha(y) - \Delta\alpha_{L0}(y) - (\alpha - \alpha_{L0})_{\text{root}}}{(\Delta\alpha - \Delta\alpha_{L0})_{\max} - (\alpha - \alpha_{L0})_{\text{root}}} \right]_{\text{twist}} \tag{8}$$

Here δ is used to signify the deflection angle for some arbitrary control surface, such as flaps or ailerons, and $\chi(y)$ specifies the spanwise control surface distribution function,

$$\chi(y) \equiv \{[\Delta\alpha(y) - \Delta\alpha_{L0}(y) - (\alpha - \alpha_{L0})_{\text{root}}]/\delta\}_{\text{control}} \tag{9}$$

For example, the case of conventional ailerons extending from the spanwise coordinate y_{ar} to y_{at}, gives the control surface distribution function

$$\chi(y) \equiv \begin{cases} 0, & y < -y_{at} \\ -\varepsilon_f(y), & -y_{at} < y < -y_{ar} \\ 0, & -y_{ar} < y < y_{ar} \\ \varepsilon_f(y), & y_{ar} < y < y_{at} \\ 0, & y > y_{at} \end{cases} \tag{10}$$

For the case of wing warping, the control surface distribution function describes the spanwise increment in local aerodynamic angle of attack relative to the undeflected wing root, which results from a unit control deflection. For a wing with more than one set of control surfaces, such as flaps and ailerons, a $\delta\chi(y)$ product term can be included in Eq. (6) for each set of controls.

Using Eqs. (2) and (6) in Eq. (3) gives

$$\sum_{n=1}^{\infty} A_n \left[\frac{4b}{\tilde{C}_{L,\alpha} c(\theta)} + \frac{n}{\sin(\theta)} \right] \sin(n\theta) = (\alpha - \alpha_{L0})_{\text{root}} - \Omega\omega(\theta) + \delta\chi(\theta) - \bar{p}\cos(\theta) \tag{11}$$

The Fourier coefficients in Eq. (11) can be conveniently written as

$$A_n = a_n(\alpha - \alpha_{L0})_{\text{root}} - b_n\Omega + c_n\delta - d_n\bar{p} \tag{12}$$

where

$$\sum_{n=1}^{\infty} a_n \left[\frac{4b}{\tilde{C}_{L,\alpha} c(\theta)} + \frac{n}{\sin(\theta)} \right] \sin(n\theta) = 1 \tag{13}$$

$$\sum_{n=1}^{\infty} b_n \left[\frac{4b}{\tilde{C}_{L,\alpha} c(\theta)} + \frac{n}{\sin(\theta)} \right] \sin(n\theta) = \omega(\theta) \tag{14}$$

$$\sum_{n=1}^{\infty} c_n \left[\frac{4b}{\tilde{C}_{L,\alpha} c(\theta)} + \frac{n}{\sin(\theta)} \right] \sin(n\theta) = \chi(\theta) \tag{15}$$

$$\sum_{n=1}^{\infty} d_n \left[\frac{4b}{\tilde{C}_{L,\alpha} c(\theta)} + \frac{n}{\sin(\theta)} \right] \sin(n\theta) = \cos(\theta) \tag{16}$$

Comparing Eq. (13) with Eq. (5), we see that the Fourier coefficients in Eq. (13) are those corresponding to the solution for a wing of the same planform shape but with no twist, control deflection, or rolling rate. The solutions to Eqs. (14–16) can be obtained in a similar manner and are all independent of angle of attack, control surface deflection, and rolling rate. Any of the methods commonly used to obtain a solution to Eq. (3) can be used to obtain the Fourier coefficients from Eqs. (13–16).

Except for the symbol used to represent the Fourier coefficients, the left-hand sides of Eqs. (13–16) are identical. Only the distribution functions on the right differ among these equations. This can be used to significant advantage in obtaining the Fourier coefficients.[19,20]

Rolling-Moment Coefficient and Roll Response

Once the Fourier coefficients are determined from Eqs. (12–16), the spanwise circulation distribution is known from Eq. (1), and the spanwise section lift distribution is given by

$$\tilde{L}(y) = \rho V_\infty \Gamma(y)$$

Thus, in view of Eqs. (1) and (2) the rolling-moment coefficient can be evaluated from

$$C_\ell = \frac{-1}{\frac{1}{2}\rho V_\infty^2 Sb} \int_{y=-b/2}^{b/2} \tilde{L}(y) y \, \mathrm{d}y = \frac{-2}{V_\infty Sb} \int_{y=-b/2}^{b/2} \Gamma(y) y \, \mathrm{d}y$$

$$= \frac{b^2}{S} \sum_{n=1}^{\infty} A_n \int_{\theta=0}^{\pi} \sin(n\theta) \cos(\theta) \sin(\theta) \, \mathrm{d}\theta$$

or after applying the definition of aspect ratio and the trigonometric identity, $\sin(2\theta) = 2\sin(\theta)\cos(\theta)$,

$$C_\ell = \frac{R_A}{2} \sum_{n=1}^{\infty} A_n \int_{\theta=0}^{\pi} \sin(n\theta) \sin(2\theta) \, \mathrm{d}\theta \tag{17}$$

The integral in Eq. (17) is evaluated from

$$\int_{\theta=0}^{\pi} \sin(m\theta) \sin(n\theta) \, \mathrm{d}\theta = \begin{cases} 0, & n \neq m \\ \pi/2, & n = m \end{cases} \tag{18}$$

After applying Eqs. (12) and (18), Eq. (17) becomes

$$C_\ell = (\pi R_A/4) A_2 = (\pi R_A/4)[a_2(\alpha - \alpha_{L0})_{\text{root}} - b_2\Omega + c_2\delta - d_2\bar{p}] \tag{19}$$

For any wing with spanwise symmetric planform and twist, the solutions to Eqs. (13) and (14) give

$$a_n = b_n = 0, \qquad n \text{ even} \tag{20}$$

and Eq. (19) reduces to

$$C_\ell = C_{\ell,\delta}\delta + C_{\ell,\bar{p}}\bar{p} \tag{21}$$

where

$$C_{\ell,\delta} = (\pi R_A/4) c_2 \tag{22}$$

$$C_{\ell,\bar{p}} = -(\pi R_A/4) d_2 \tag{23}$$

The Fourier coefficients obtained from Eq. (15) depend on control surface geometry as well as the planform shape of the wing. However, the Fourier coefficients evaluated from Eq. (16) are only functions of wing planform. For an elliptic planform, the spanwise variation in chord length is given by

$$c(y) = (4b/\pi R_A)\sqrt{1 - (2y/b)^2} \quad \text{or} \quad c(\theta) = (4b/\pi R_A)\sin(\theta) \tag{24}$$

and Eq. (16) reduces to

$$\sum_{n=1}^{\infty} d_n \left(\frac{\pi R_A}{\tilde{C}_{L,\alpha}} + n \right) \sin(n\theta) = \sin(\theta)\cos(\theta) \tag{25}$$

After applying the identity, $2\sin(\theta)\cos(\theta) = \sin(2\theta)$, the solution to Eq. (25) is

$$d_n \left(\frac{\pi R_A}{\tilde{C}_{L,\alpha}} + n \right) = \frac{2}{\pi} \int_0^{\pi} \sin(\theta)\cos(\theta)\sin(n\theta) \, \mathrm{d}\theta$$

$$= \frac{1}{\pi} \int_0^{\pi} \sin(2\theta)\sin(n\theta) \, \mathrm{d}\theta$$

which is readily evaluated from Eq. (18) to yield

$$d_n = \begin{cases} \dfrac{\tilde{C}_{L,\alpha}}{2(\pi R_A + 2\tilde{C}_{L,\alpha})}, & n = 2 \\ 0, & n \neq 2 \end{cases} \tag{26}$$

Using Eq. (26) in Eq. (23) gives

$$C_{\ell,\bar{p}} = \frac{-\tilde{C}_{L,\alpha}}{8(1 + 2\tilde{C}_{L,\alpha}/\pi R_A)} \tag{27}$$

The lift slope for a wing of elliptic planform is given by

$$C_{L,\alpha} = \frac{\tilde{C}_{L,\alpha}}{1 + \tilde{C}_{L,\alpha}/\pi R_A} \tag{28}$$

Thus, in view of Eqs. (27) and (28) the change in rolling-moment coefficient with respect to dimensionless rolling rate for an elliptic wing can be written as

$$C_{\ell,\bar{p}} = -\frac{\kappa_{\ell\bar{p}} C_{L,\alpha}}{8}, \qquad \kappa_{\ell\bar{p}} \equiv \frac{1 + \tilde{C}_{L,\alpha}/\pi R_A}{1 + 2\tilde{C}_{L,\alpha}/\pi R_A} \tag{29}$$

The lift slope for a wing of arbitrary planform is independent of twist[19,20] and is given by

$$C_{L,\alpha} = \pi R_A a_1 \tag{30}$$

For the general case of a wing with arbitrary planform and twist, combining Eqs. (23) and (30) gives

$$C_{\ell,\bar{p}} = -(\kappa_{\ell\bar{p}} C_{L,\alpha}/8), \quad \kappa_{\ell\bar{p}} \equiv 2d_2/a_1 \tag{31}$$

For an airfoil-section lift slope of 2π, results for tapered wings are shown in Fig. 2.

One significant measure of an airplane's roll response is the change in equilibrium dimensionless rolling rate with respect to control surface deflection. From Eq. (21), the equilibrium dimensionless rolling rate that results in no rolling moment is given by

$$\bar{p}_0 = -(C_{\ell,\delta}/C_{\ell,\bar{p}})\delta \tag{32}$$

and in view of Eqs. (22) and (23), the roll response derivative is

$$\frac{\partial \bar{p}_0}{\partial \delta} = -\frac{C_{\ell,\delta}}{C_{\ell,\bar{p}}} = \frac{c_2}{d_2} \tag{33}$$

which is independent of both angle of attack and the spanwise symmetric wing twist.

Yawing-Moment Coefficient and Adverse Yaw

The spanwise variations in aerodynamic angle of attack, which result from asymmetric control surface deflection and roll, also

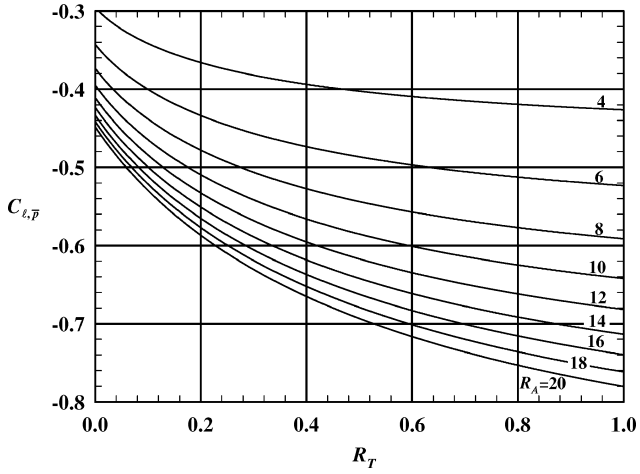

Fig. 2 Roll-damping derivative for wings with linear taper and arbitrary twist.

produce a yawing moment. This yawing moment develops as a direct result of an asymmetric spanwise variation in induced drag. Thus, the yawing-moment coefficient can be written as

$$C_n = \frac{1}{\frac{1}{2}\rho V_\infty^2 Sb}\int_{y=-b/2}^{b/2} \tilde{D}_i(y)\, y\, \mathrm{d}y \tag{34}$$

The section induced drag results from the tilting of the section lift vector through the induced angle α_i and the roll angle $-yp/V_\infty$. Thus, after expressing the section lift in terms of the section circulation we have

$$\tilde{D}_i(y) = \tilde{L}\sin(\alpha_i - yp/V_\infty) \cong \tilde{L}(\alpha_i - yp/V_\infty)$$

$$= \rho V_\infty \Gamma(y)[\alpha_i(y) - yp/V_\infty] \tag{35}$$

The induced angle of attack as predicted by lifting-line theory is[7–11]

$$\alpha_i(y) = \frac{1}{4\pi V_\infty}\int_{\zeta=-b/2}^{b/2} \frac{1}{y-\zeta}\left(\frac{\mathrm{d}\Gamma}{\mathrm{d}y}\right)_{y=\zeta} \mathrm{d}\zeta \tag{36}$$

Using Eqs. (35) and (36) in Eq. (34) gives

$$C_n = \int_{y=-b/2}^{b/2} \frac{2y\Gamma(y)}{V_\infty^2 Sb}\left[\frac{1}{4\pi}\int_{\zeta=-b/2}^{b/2}\frac{1}{y-\zeta}\left(\frac{\mathrm{d}\Gamma}{\mathrm{d}y}\right)_{y=\zeta}\mathrm{d}\zeta - yp\right]\mathrm{d}y \tag{37}$$

From Eqs. (1) and (2) we have

$$\Gamma(\theta) = 2bV_\infty \sum_{n=1}^{\infty} A_n \sin(n\theta)$$

$$\cos(\theta) = -\frac{2y}{b}, \qquad \frac{\mathrm{d}\theta}{\mathrm{d}y} = \frac{2}{b\sin(\theta)}$$

$$\frac{\mathrm{d}\Gamma}{\mathrm{d}y} = 4V_\infty \sum_{n=1}^{\infty} A_n \frac{n\cos(n\theta)}{\sin(\theta)}$$

and Eq. (37) can be written as

$$C_n = \frac{-b^2}{\pi S}\int_{\theta=0}^{\pi}\cos(\theta)\left[\sum_{n=1}^{\infty} A_n \sin(n\theta)\right]$$

$$\times\left[\sum_{n=1}^{\infty} nA_n \int_{\phi=0}^{\pi}\frac{\cos(n\phi)}{\cos(\phi)-\cos(\theta)}\mathrm{d}\phi\right]\sin(\theta)\,\mathrm{d}\theta$$

$$-\frac{b^2\bar{p}}{S}\sum_{n=1}^{\infty} A_n \int_{\theta=0}^{\pi}\cos^2(\theta)\sin(\theta)\sin(n\theta)\,\mathrm{d}\theta \tag{38}$$

The integration with respect to ϕ yields

$$\int_{\phi=0}^{\pi}\frac{\cos(n\phi)}{\cos(\phi)-\cos(\theta)}\mathrm{d}\phi = \frac{\pi\sin(n\theta)}{\sin(\theta)} \tag{39}$$

Thus, applying the identity $\sin(2\theta) = 2\sin(\theta)\cos(\theta)$ the yawing-moment coefficient for a wing of arbitrary planform can be evaluated from

$$C_n = -R_A \sum_{n=1}^{\infty}\sum_{m=1}^{\infty} nA_nA_m \int_{\theta=0}^{\pi}\cos(\theta)\sin(n\theta)\sin(m\theta)\,\mathrm{d}\theta$$

$$-R_A\bar{p}\sum_{n=1}^{\infty} A_n \frac{1}{2}\int_{\theta=0}^{\pi}\cos(\theta)\sin(2\theta)\sin(n\theta)\,\mathrm{d}\theta \tag{40}$$

Because m and n are positive integers, the integrals with respect to θ are evaluated from

$$\int_{\theta=0}^{\pi}\cos(\theta)\sin(n\theta)\sin(m\theta)\,\mathrm{d}\theta = \begin{cases}\dfrac{\pi}{4}, & m = n\pm 1\\ 0, & m \neq n\pm 1\end{cases} \tag{41}$$

and after some rearranging we obtain

$$C_n = -\frac{\pi R_A}{4}\sum_{n=2}^{\infty}(2n-1)A_{n-1}A_n - \frac{\pi R_A\bar{p}}{8}(A_1 + A_3) \tag{42}$$

The lift coefficient predicted by lifting-line theory is[7–11]

$$C_L = \pi R_A A_1 \tag{43}$$

After applying Eq. (43) to Eq. (42), we find that the yawing-moment coefficient is given by

$$C_n = -\frac{C_L}{8}(6A_2 + \bar{p}) - \frac{\pi R_A}{8}(10A_2 + \bar{p})A_3$$

$$-\frac{\pi R_A}{4}\sum_{n=4}^{\infty}(2n-1)A_{n-1}A_n \tag{44}$$

where the Fourier coefficients A_n are related to angle of attack, wing twist, control surface deflection, and rolling rate through Eq. (12).

If $c(\theta)$ and $\omega(\theta)$ are both spanwise symmetric, all even coefficients in both a_n and b_n are zero. The change in aerodynamic angle of attack that results from roll is always spanwise odd. Thus, all odd coefficients in d_n are zero for a spanwise symmetric wing. If the control surfaces are conventional ailerons that produce an equal and opposite change on each semispan, the control surface distribution function is a spanwise odd function as well, and all odd coefficients in c_n are also zero. With this wing symmetry, the Fourier coefficients must satisfy the relations $a_n = b_n = 0$ for n even and $c_n = d_n = 0$ for n odd. Thus, Eq. (12) reduces to

$$A_n = \begin{cases} a_n(\alpha - \alpha_{L0})_{\text{root}} - b_n\Omega, & n \text{ odd}\\ c_n\delta - d_n\bar{p}, & n \text{ even}\end{cases} \tag{45}$$

Using the Fourier coefficients from Eq. (45) in Eq. (44), the yawing-moment coefficient with the wing symmetry just described is given by

$$C_n = -\frac{C_L}{8}[6c_2\delta + (1-6d_2)\bar{p}]$$

$$-\frac{\pi R_A}{4}\left\{\frac{1}{2}[10c_2\delta + (1-10d_2)\bar{p}][a_3(\alpha-\alpha_{L0})_{\text{root}} - b_3\Omega]\right.$$

$$+\sum_{\substack{n=4\\ n\text{ even}}}^{\infty}(2n-1)[a_{n-1}(\alpha-\alpha_{L0})_{\text{root}} - b_{n-1}\Omega](c_n\delta - d_n\bar{p})$$

$$\left.+\sum_{\substack{n=5\\ n\text{ odd}}}^{\infty}(2n-1)(c_{n-1}\delta - d_{n-1}\bar{p})[a_n(\alpha-\alpha_{L0})_{\text{root}} - b_n\Omega]\right\} \tag{46}$$

For the special case of a symmetric wing operating with optimum twist, $a_n(\alpha - \alpha_{L0})_{\text{root}} - b_n\Omega$ is always exactly zero for all n greater than one.[19,20] Thus, the yawing-moment coefficient for symmetric wings with optimum twist can be written as

$$C_n = C_{n,\delta}\delta + C_{n,\bar{p}}\bar{p} \tag{47}$$

where

$$C_{n,\delta} = -(3C_L/4)c_2 \tag{48}$$

$$C_{n,\bar{p}} = -C_L/8(1 - 6d_2) \tag{49}$$

By comparing Eqs. (21–23) with Eqs. (47–49), we see that for symmetric wings with optimum twist the yawing-moment coefficient can be expressed in terms of the rolling-moment coefficient and the dimensionless rolling rate:

$$C_n = -(3C_L/\pi R_A)C_\ell - (C_L/8)\bar{p} \tag{50}$$

For typical symmetric wings without optimum twist, the higher-order terms in Eq. (46) are not too large, and the linear relation from either Eq. (47) or (50) can be used as a rough approximation. For example, consider a rectangular wing of aspect ratio 8.0 having ailerons with sealed hinges that extend from the spanwise coordinate $y/b = \pm 0.25$ to ± 0.45. The aileron chord length is constant and equal to 18% of the wing chord, and the section flap effectiveness is constant and equal to 0.445. The wing is operating at the design lift coefficient of 0.4, and there is no rolling rate. If optimum twist is assumed, carrying 99 terms in the infinite series and assuming an airfoil-section lift slope of 2π gives a yawing-moment coefficient of $C_n = 0.00101$ for a 5-deg aileron deflection. This result strictly applies only to a wing with optimum twist, which in this case requires 4.64 deg of elliptic washout. For the same wing planform with no twist, carrying the higher-order terms using either Eq. (44) or (46) gives $C_n = 0.00123$ and with 4.5 deg of linear washout we get $C_n = 0.00087$. The contribution of the higher-order terms in Eqs. (44) and (46) is typically on the order of 10 to 25%.

Minimizing Induced Drag with Control Surface Twist

In addition to using trailing-edge flaps for roll control and high-lift devices, it is possible to use variable twist in trailing-edge flaps to minimize induced drag. The induced drag predicted from lifting-line theory is given by[7–11]

$$C_{Di} = \pi R_A \sum_{n=1}^{\infty} n A_n^2 \tag{51}$$

Using Eqs. (12) and (43) in Eq. (51), the induced drag can be expressed as

$$C_{Di} = \frac{C_L^2}{\pi R_A} + \pi R_A \sum_{n=2}^{\infty} n[a_n(\alpha - \alpha_{L0})_{\text{root}} - b_n\Omega + c_n\delta - d_n\bar{p}]^2 \tag{52}$$

where

$$C_L = \pi R_A[a_1(\alpha - \alpha_{L0})_{\text{root}} - b_1\Omega + c_1\delta - d_1\bar{p}] \tag{53}$$

Induced drag is minimized for a given lift coefficient and aspect ratio when

$$a_n(\alpha - \alpha_{L0})_{\text{root}} - b_n\Omega + c_n\delta - d_n\bar{p} = 0, \quad \text{for } n \neq 1 \tag{54}$$

With no control deflection or rolling rate, minimum induced drag can always be maintained if wing twist is related to wing planform and lift coefficient according to the relations presented by Phillips[19,20]:

$$\omega(y) = 1 - \frac{\sqrt{1 - (2y/b)^2}}{c(y)/c_{\text{root}}} \quad \text{or} \quad \omega(\theta) = 1 - \frac{\sin(\theta)}{c(\theta)/c_{\text{root}}} \tag{55}$$

$$\Omega_{\text{opt}} = \frac{\kappa_{DL}C_L}{2\kappa_{D\Omega}C_{L,\alpha}} \tag{56}$$

$$\kappa_{DL} \equiv 2\frac{b_1}{a_1}\sum_{n=2}^{\infty} n\frac{a_n}{a_1}\left(\frac{b_n}{b_1} - \frac{a_n}{a_1}\right) \tag{57}$$

$$\kappa_{D\Omega} \equiv \left(\frac{b_1}{a_1}\right)^2 \sum_{n=2}^{\infty} n\left(\frac{b_n}{b_1} - \frac{a_n}{a_1}\right)^2 \tag{58}$$

With this spanwise variation in washout, an unswept wing of any planform produces the same minimum induced drag as an unswept elliptic wing having the same aspect ratio and lift coefficient.

A wing with linear taper has a chord that varies with the spanwise coordinate according to the relation

$$c(y) = \frac{2b}{R_A(1 + R_T)}\left[1 - (1 - R_T)\left|\frac{2y}{b}\right|\right]$$

$$\text{or} \quad c(\theta) = \frac{2b}{R_A(1 + R_T)}[1 - (1 - R_T)\,|\cos(\theta)|] \tag{59}$$

For this planform, the optimum washout distribution function $\omega(y)$ is shown in Fig. 3 for several values of taper ratio. Using Eqs. (55) and (59) in Eqs. (13) and (14) yields

$$\sum_{n=1}^{\infty}\frac{a_n}{a_1}\sin(n\theta) + \frac{\tilde{C}_{L,\alpha}[1 - (1 - R_T)\,|\cos(\theta)|]}{2R_A(1 + R_T)}\sum_{n=1}^{\infty} n\frac{a_n}{a_1}\frac{\sin(n\theta)}{\sin(\theta)}$$

$$= \frac{\tilde{C}_{L,\alpha}[1 - (1 - R_T)\,|\cos(\theta)|]}{2a_1R_A(1 + R_T)} \tag{60}$$

$$\sum_{n=1}^{\infty}\frac{b_n}{b_1}\sin(n\theta) + \frac{\tilde{C}_{L,\alpha}[1 - (1 - R_T)\,|\cos(\theta)|]}{2R_A(1 + R_T)}\sum_{n=1}^{\infty} n\frac{b_n}{b_1}\frac{\sin(n\theta)}{\sin(\theta)}$$

$$= \frac{\tilde{C}_{L,\alpha}[1 - \sin(\theta) - (1 - R_T)\,|\cos(\theta)|]}{2b_1R_A(1 + R_T)} \tag{61}$$

To evaluate the induced drag for this wing, we make use of the Fourier expansions for $0 \leq \theta \leq \pi$,

$$1 = \frac{2}{\pi}\left[2\sin(\theta) + \sum_{m=1}^{\infty}\frac{2}{2m+1}\sin[(2m+1)\theta]\right] \tag{62}$$

$$|\cos(\theta)| = \frac{2}{\pi}\left[\sin(\theta) + \sum_{m=1}^{\infty}\frac{2m + 1 - (-1)^m}{2m(m+1)}\sin[(2m+1)\theta]\right] \tag{63}$$

and the trigonometric identities,

$$\frac{\sin[(2m+1)\theta]}{\sin(\theta)} = \frac{\sin[(2m-1)\theta]}{\sin(\theta)} + 2\cos(2m\theta) \tag{64}$$

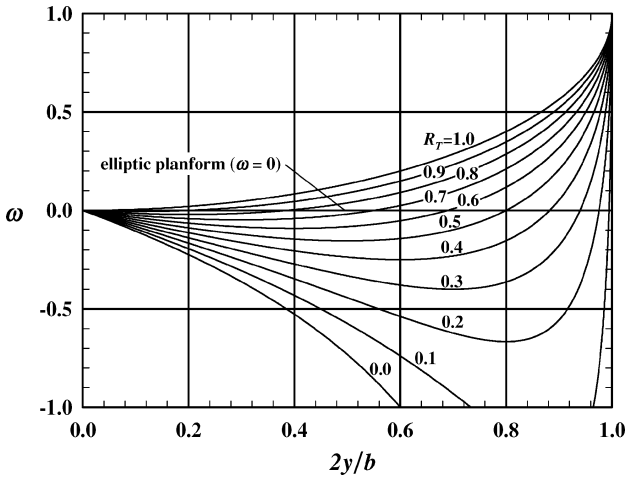

Fig. 3 Optimum washout distribution for wings with linear taper.

$$2\cos(2m\theta)\sin[(2n+1)\theta] = \sin[(2m+2n+1)\theta] - \sin[(2m-2n-1)\theta] \tag{65}$$

By using Eqs. (62–65) in Eqs. (60) and (61), equating the coefficients of $\sin(n\theta)$ from both sides of these equations, and applying the results to Eqs. (57) and (58), we find that an unswept wing with linear taper and the washout distribution specified by Eq. (55) results in

$$\kappa_{DL} \equiv 2\frac{b_1}{a_1}\sum_{n=2}^{\infty} n\frac{a_n}{a_1}\left(\frac{b_n}{b_1}-\frac{a_n}{a_1}\right) = \frac{\tilde{C}_{L,\alpha}}{R_A(1+R_T)}\sum_{n=2}^{\infty} n\frac{a_n^2}{a_1^3} \tag{66}$$

$$\kappa_{D\Omega} \equiv \left(\frac{b_1}{a_1}\right)^2\sum_{n=2}^{\infty} n\left(\frac{b_n}{b_1}-\frac{a_n}{a_1}\right)^2 = \frac{\tilde{C}_{L,\alpha}^2}{4R_A^2(1+R_T)^2}\sum_{n=2}^{\infty} n\frac{a_n^2}{a_1^4} \tag{67}$$

With no control deflection or rolling rate, Eq. (52) can be rearranged to yield

$$C_{Di} = \frac{C_L^2}{\pi R_A} + \pi R_A[a_1(\alpha-\alpha_{L0})_{\text{root}} - b_1\Omega]^2\sum_{n=2}^{\infty} n\frac{a_n^2}{a_1^2} - 2\pi R_A[a_1(\alpha-\alpha_{L0})_{\text{root}} - b_1\Omega]b_1\Omega\sum_{n=2}^{\infty} n\frac{a_n}{a_1}\left(\frac{b_n}{b_1}-\frac{a_n}{a_1}\right) + \pi R_A b_1^2\Omega^2\sum_{n=2}^{\infty} n\left(\frac{b_n}{b_1}-\frac{a_n}{a_1}\right)^2 \tag{68}$$

or in view of Eq. (53)

$$C_{Di} = \frac{C_L^2}{\pi R_A}\left(1+\sum_{n=2}^{\infty} n\frac{a_n^2}{a_1^2}\right) - 2C_L b_1\Omega\sum_{n=2}^{\infty} n\frac{a_n}{a_1}\left(\frac{b_n}{b_1}-\frac{a_n}{a_1}\right) + \pi R_A b_1^2\Omega^2\sum_{n=2}^{\infty} n\left(\frac{b_n}{b_1}-\frac{a_n}{a_1}\right)^2 \tag{69}$$

Applying Eqs. (66) and (67) to Eq. (69), with no control deflection or rolling rate the induced drag for a wing with linear taper and the optimum washout distribution obtained from Eq. (55) can be written as

$$C_{Di} = \frac{C_L^2}{\pi R_A} + \frac{1}{\pi R_A}\sum_{n=2}^{\infty} n\frac{a_n^2}{a_1^2}\left[C_L - \frac{\pi\tilde{C}_{L,\alpha}\Omega}{2(1+R_T)}\right]^2 \tag{70}$$

From Eq. (70), we see that any wing with linear taper and the corresponding optimum washout distribution specified by Eq. (55) produces the same minimum induced drag as an elliptic wing with no twist, provided that the total washout is related to the lift coefficient according to

$$\Omega_{\text{opt}} = \frac{2(1+R_T)C_L}{\pi\tilde{C}_{L,\alpha}} \tag{71}$$

The wing twist defined by Eqs. (55–58) can be used to maintain minimum induced drag over a range of operating conditions by employing full-span trailing-edge flaps that can be twisted along their length to produce a continuous spanwise variation in zero-lift angle of attack. For a rectangular wing, Eq. (55) requires little twist in the region near the root. Thus, the geometry shown in Fig. 4 can be used to closely approximate the aerodynamic twist needed to minimize induced drag. In the following discussion, the twisting control surfaces shown in Fig. 4 are referred to as *twisterons*. The rectangular wing shown in Fig. 4 has an aspect ratio of 6.0 with 30% trailing-edge flaps that provide a section flap effectiveness of 0.60. For an airfoil-section lift slope of 2π and a lift coefficient of 0.60, Eqs. (55) and (71) require a spanwise elliptic washout distribution with 7.0 deg of total washout at the wingtips. Because the section flap effectiveness is 0.60, this requires 11.6 deg of elliptic flap twist, which is shown in Fig. 4a. Similarly, a lift coefficient of 1.40 requires 27.1 deg of elliptic flap twist, which is shown in Fig. 4b in combination with 15-deg flap deflection. These control surfaces can also be deflected asymmetrically as ailerons to establish roll control. An experimental radio-controlled aircraft with operational twisterons is shown in Fig. 5.

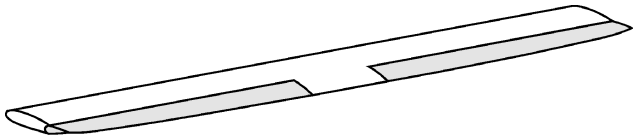

a) Twisteron configuration with no flap deflection and washout set to minimize induced drag at $C_L = 0.6$.

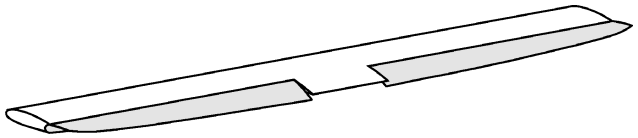

b) Twisteron configuration with 15° flap deflection and washout set to minimize induced drag at $C_L = 1.4$.

Fig. 4 Rectangular wing fitted with 30% constant-chord twisterons to produce variable elliptic washout.

Fig. 5 Experimental aircraft with operational twisterons.

As an example, consider an untwisted rectangular wing with full-span constant-chord twisterons, which can be twisted along their length to produce a spanwise elliptic washout distribution. These control surfaces can also be deflected as flaps and/or ailerons. Because section flap effectiveness does not vary along the span of this wing, the spanwise variation in aerodynamic angle of attack with respect to the freestream can be written in the same form as Eq. (6):

$$\alpha(y) - \alpha_{L0}(y) \equiv (\alpha-\alpha_{L0})_{\text{ref}} + \varepsilon_f\delta_f - \varepsilon_f\delta_t\left[1-\sqrt{1-(2y/b)^2}\right] + \varepsilon_f\delta_a(y/|y|) + py/V_\infty \tag{72}$$

where the subscript ref denotes the base airfoil section with no control deflection. Using Eq. (72) in Eq. (3) with the change of variables defined in Eq. (2) yields

$$\sum_{n=1}^{\infty} A_n\left[\frac{4R_A}{\tilde{C}_{L,\alpha}} + \frac{n}{\sin(\theta)}\right]\sin(n\theta) = (\alpha-\alpha_{L0})_{\text{ref}} + \varepsilon_f\delta_f - \varepsilon_f\delta_t[1-\sin(\theta)] + \varepsilon_f\delta_a[-\cos(\theta)/|\cos(\theta)|] - \bar{p}\cos(\theta) \tag{73}$$

The Fourier coefficients in Eq. (73) can be written as

$$A_n = a_n[(\alpha-\alpha_{L0})_{\text{ref}} + \varepsilon_f\delta_f] - b_n\varepsilon_f\delta_t + c_n\varepsilon_f\delta_a - d_n\bar{p} \tag{74}$$

where

$$\sum_{n=1}^{\infty} a_n \left[\frac{4R_A}{\tilde{C}_{L,\alpha}} + \frac{n}{\sin(\theta)} \right] \sin(n\theta) = 1 \tag{75}$$

$$\sum_{n=1}^{\infty} b_n \left[\frac{4R_A}{\tilde{C}_{L,\alpha}} + \frac{n}{\sin(\theta)} \right] \sin(n\theta) = 1 - \sin(\theta) \tag{76}$$

$$\sum_{n=1}^{\infty} c_n \left[\frac{4R_A}{\tilde{C}_{L,\alpha}} + \frac{n}{\sin(\theta)} \right] \sin(n\theta) = \begin{cases} -1, & 0 \le \theta \le \pi/2 \\ +1, & \pi/2 \le \theta \le \pi \end{cases} \tag{77}$$

$$\sum_{n=1}^{\infty} d_n \left[\frac{4R_A}{\tilde{C}_{L,\alpha}} + \frac{n}{\sin(\theta)} \right] \sin(n\theta) = \cos(\theta) \tag{78}$$

The Fourier coefficients a_n are exactly those obtained from Eq. (5) for a wing of the same planform geometry without geometric or aerodynamic twist. The remaining Fourier coefficients b_n, c_n, and d_n can be obtained from Eqs. (76–78) in a similar manner.

As seen in Eq. (43), the lift coefficient predicted from lifting-line theory depends only on the first Fourier coefficient A_1. Because the right-hand sides of Eqs. (77) and (78) are odd functions of the spanwise coordinate over the range $0 \le \theta \le \pi$, the solutions yield $c_n = d_n = 0$ for all odd values of n. Using Eq. (74) in Eq. (43), the lift coefficient for a rectangular wing with full-span constant-chord twisterons is predicted to be

$$C_L = \pi R_A a_1 [(\alpha - \alpha_{L0})_{\text{ref}} + \varepsilon_f \delta_f] - \pi R_A b_1 \varepsilon_f \delta_t \tag{79}$$

The twisterons provide the only spanwise symmetric twist in this wing, that is, $\Omega = \varepsilon_f \delta_t$. Thus, from Eq. (70) the induced drag coefficient for this rectangular wing, with no aileron deflection or roll, can be written as

$$C_{Di} = \frac{C_L^2}{\pi R_A} + \frac{1}{\pi R_A} \sum_{n=2}^{\infty} n \frac{a_n^2}{a_1^2} \left(C_L - \frac{\pi \tilde{C}_{L,\alpha} \varepsilon_f}{4} \delta_t \right)^2 \tag{80}$$

and the total twisteron deflection required to minimize induced drag at any given lift coefficient is

$$(\delta_t)_{\text{opt}} = \frac{4C_L}{\pi \tilde{C}_{L,\alpha} \varepsilon_f} \tag{81}$$

Because the right-hand sides of Eqs. (75) and (76) are spanwise even functions over the range $0 \le \theta \le \pi$, the solutions result in $a_n = b_n = 0$ all for even values of n. Thus, from Eqs. (19) and (74), the rolling-moment coefficient predicted for this wing geometry is

$$C_\ell = (\pi R_A c_2 \varepsilon_f / 4) \delta_a - (\pi R_A d_2 / 4) \bar{p} \tag{82}$$

It should be noted from Eqs. (75–82) that several of the important aerodynamic derivatives for this wing geometry depend only on aspect ratio and airfoil-section lift slope,

$$C_{L,\delta_f} / \varepsilon_f = C_{L,\alpha} = \pi R_A a_1 \tag{83}$$

$$C_{L,\delta_t} / \varepsilon_f = -\pi R_A b_1 \tag{84}$$

$$C_{\ell,\delta_a} / \varepsilon_f = \pi R_A c_2 / 4 \tag{85}$$

$$C_{\ell,\bar{p}} = -\pi R_A d_2 / 4 \tag{86}$$

For an airfoil-section lift slope of 2π, these aerodynamic derivatives are shown as a function of aspect ratio in Fig. 6.

Another advantage of using twisterons to minimize induced drag produced by the main wing of an airplane is a reduction in the up-elevator deflection required for trim at high lift coefficients. When twisteron deflection varies with lift coefficient in accordance with Eqs. (55) and (71), the pitching moment produced by the wing becomes more positive as the lift coefficient and twisteron deflection are increased. This reduces the negative lift on the horizontal stabilizer, which is typically required for high lift coefficients, and

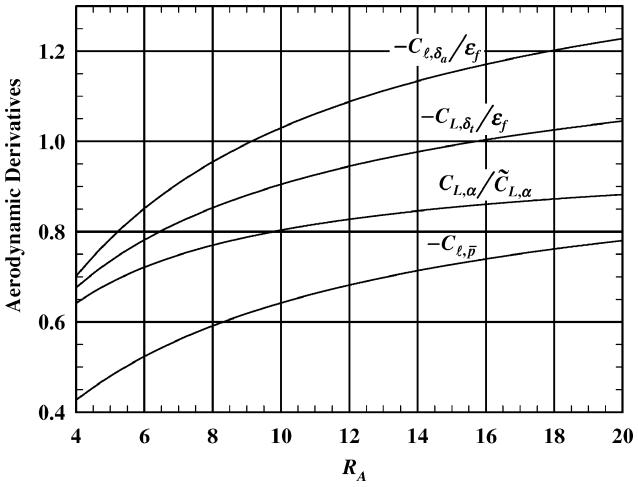

Fig. 6 Aerodynamic derivatives for a rectangular wing with full-span constant-chord twisterons.

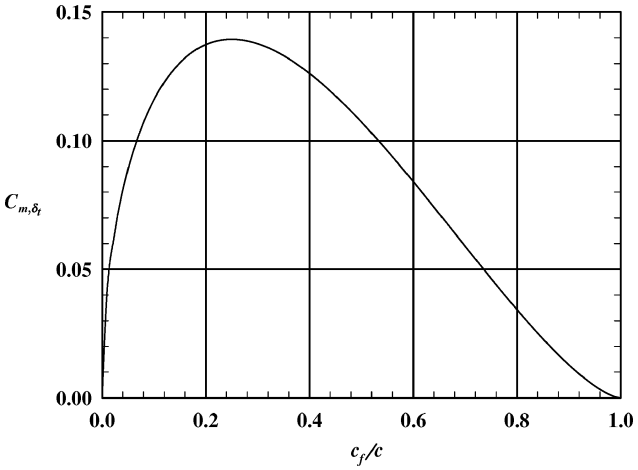

Fig. 7 Change in pitching-moment coefficient with respect to twisteron deflection.

provides additional savings in drag over that realized for the wing alone. For example, consider again the rectangular wing with full-span constant-chord twisterons described in Eq. (72). The change in wing pitching-moment coefficient with respect to twisteron deflection for this wing geometry is evaluated from

$$C_{m,\delta_t} \equiv \frac{\partial C_m}{\partial \delta_t} = -\frac{1}{b} \int_{-b/2}^{b/2} \tilde{C}_{m,\delta} \left[1 - \sqrt{1 - (2y/b)^2} \right] \mathrm{d}y \tag{87}$$

Because the change in section moment coefficient with flap deflection is constant for this wing geometry, the integral in Eq. (87) can be evaluated to give

$$C_{m,\delta_t} = -\tilde{C}_{m,\delta}(1 - \pi/4) \tag{88}$$

If the airfoil-section moment coefficient is evaluated from thin airfoil theory,[21] this result can be written in terms of the section flap fraction:

$$C_{m,\delta_t} = (2 - \pi/2) \sqrt{(c_f/c)(1 - c_f/c)^3} \tag{89}$$

Results predicted from this relation are shown in Fig. 7.

Conclusions

When the classical form of the lifting-line solution is used for wings with twist, control surface deflection, or rolling rate, the Fourier coefficients in the infinite series all depend on angle of attack and other operating conditions. Because these coefficients must

be reevaluated for each operating point, this form of the solution is cumbersome for evaluating wing properties. A more practical form of the lifting-line solution for finite wings has been presented. This solution is based on a change of variables, which allows the infinite series to be divided into four parts that separately account for wing planform, wing twist, control surface deflection, and rolling rate. The Fourier coefficients in all four of these infinite series depend only on wing geometry and can be evaluated independent of angle of attack, control surface deflection, and rolling rate. In addition to predicting lift and induced drag, the solution can be used to predict the rolling and yawing moments that result from control surface deflection and rolling rate.

The present form of the lifting-line solution shows that, in addition to using trailing-edge flaps for roll control and high lift, it is possible to use variable twist in trailing-edge flaps to minimize induced drag. Minimum induced drag can be maintained over a wide range of operating conditions by employing full-span trailing-edge flaps that can be twisted along their length to produce a continuous spanwise variation in zero-lift angle of attack. In the present paper, such twisting control surfaces were referred to as twisterons. An analytical solution was presented for the optimum spanwise twist distribution that results in minimum induced drag for a wing of arbitrary planform. For the case of a tapered wing, this solution was presented in closed form. When twisterons are used to maintain this optimum twist, a wing of any planform produces the same minimum induced drag as an untwisted elliptic wing.

Acknowledgments

The authors would like to thank Mark E. Anderson, Kyle M. Barton, Nathan E. Bunderson, Michael J. Okseness, Adam G. Spinner, David M. Stuart, and Tristan L. Young for the many hours of work invested in designing, building, and testing of the experimental aircraft.

References

[1]Prandtl, L., "Tragflügel Theorie," *Nachricten von der Gesellschaft der Wissenschaften zu Göttingen*, Geschäeftliche Mitteilungen, Klasse, Germany, 1918, pp. 451–477.

[2]Prandtl, L., "Applications of Modern Hydrodynamics to Aeronautics," NACA TR-116, June 1921.

[3]Glauert, H., "The Monoplane Aerofoil," *The Elements of Aerofoil and Airscrew Theory*, Cambridge Univ. Press, Cambridge, England, UK, 1926, pp. 137–155.

[4]Multhopp, H., "Die Berechnung der Auftriebs Verteilung von Tragflugeln," *Luftfahrtforschung*, Vol. 15, No. 14, 1938, pp. 153–169.

[5]Lotz, I., "Berechnung der Auftriebsverteilung Beliebig Geformter Flugel," *Zeitschrift für Flugtechnik und Motorluftschiffahrt*, Vol. 22, No. 7, 1931, pp. 189–195.

[6]Karamcheti, K., "Elements of Finite Wing Theory," *Ideal-Fluid Aerodynamics*, Wiley, New York, 1966, pp. 535–567.

[7]Bertin, J. J., "Incompressible Flow About Wings of Finite Span," *Aerodynamics for Engineers*, 4th ed., Prentice–Hall, Upper Saddle River, NJ, 2002, pp. 230–302.

[8]Anderson, J. D., "Incompressible Flow over Finite Wings: Prandtl's Classical Lifting-Line Theory," *Fundamentals of Aerodynamics*, 3rd ed., McGraw–Hill, New York, 1991, pp. 360–387.

[9]Katz, J., and Plotkin, A., "Finite Wing: The Lifting-Line Model," *Low-Speed Aerodynamics*, 2nd ed., Cambridge Univ. Press, Cambridge, England, U.K., 2001, pp. 167–183.

[10]Kuethe, A. M., and Chow, C. Y., "The Finite Wing," *Foundations of Aerodynamics*, 5th ed., Wiley, New York, 1998, pp. 169–219.

[11]McCormick, B. W., "The Lifting Line Model," *Aerodynamics, Aeronautics, and Flight Mechanics*, 2nd ed., Wiley, New York, 1995, pp. 112–119.

[12]Munk, M. M., "On the Distribution of Lift Along the Span of an Airfoil with Displaced Ailerons," NACA TN-195, June 1924.

[13]Munk, M. M., "A New Relation Between the Induced Yawing Moment and the Rolling Moment of an Airfoil in Straight Motion," NACA TR-197, June 1925.

[14]Glauert, H., "Theoretical Relationships for an Airfoil with Hinged Flap," Aeronautical Research Council, Reports and Memoranda 1095, London, July 1927.

[15]Hartshorn, A. S., "Theoretical Relationship for a Wing with Unbalanced Ailerons," Aeronautical Research Council, Reports and Memoranda 1259, London, Oct. 1929.

[16]Pearson, H. A., "Theoretical Span Loading and Moments of Tapered Wings Produced by Aileron Deflection," NACA TN-589, Jan. 1937.

[17]Pearson, H. A., "Span Load Distribution for Tapered Wings with Partial-Span Flaps," NACA TR-585, Nov. 1937.

[18]Pearson, H. A., and Jones, R. T., "Theoretical Stability and Control Characteristics of Wings with Various Amounts of Taper and Twist," NACA TR-635, April 1937.

[19]Phillips, W. F., "Lifting-Line Analysis for the Effects of Washout on Performance and Stability," AIAA Paper 2003-0393, Jan. 2003.

[20]Phillips, W. F., "Lifting-Line Analysis for Twisted Wings and Washout-Optimized Wings," *Journal of Aircraft*, Vol. 41, No. 1, 2004, pp. 128–136.

[21]Kuethe, A. M., and Chow, C. Y., "The Flapped Airfoil," *Foundations of Aerodynamics*, 5th ed., Wiley, New York, 1998, pp. 150–154.